Design and Research of Axial Flux Permanent Magnet Motor for Electric Vehicle

Huang Qi
Northwestern Polytechnical University
School of Automation
Xi'an, China
Email: snk77@163.com

Luo Ling
Northwestern Polytechnical University
School of Automation
Xi'an, China

Zhu Liwei
National Engineering Research Center
for Small and Special Precision
Guiyang, China

2019 IEEE 3rd International Electrical and Energy Conference (CIEEC) 978-1-7281-1675-4/20/$31.00 ©2020 IEEE 10.1109/CIEEC47146.2019.CIEEC-2019658

***Abstract*—Electric drive system improves the operation performance of electric vehicles, but brings high technical requirements of the motor. This paper proposes an axial flux permanent magnet near-wheel motor with double stator and single rotor structure for electric vehicle. Focusing on the purpose of reducing the THD of back electromotive force, reducing torque pulsation and rotor eddy current loss, the stator slot type, pole-slot combination, skewed permanent magnet and segments of permanent magnet are analyzed. In order to realize high overload capacity, the spiral channel heat dissipation design is presented. In addition, the weight reduction design is carried out on the front and rear end cover, shell and rotating shaft of the motor. Meanwhile the strength analysis and modal analysis are finished by FEA tools. Finally, a prototype of the axial magnetic flux permanent magnet motor was produced, and an experimental platform was built to test the efficiency characteristics, magnetic field weakening properties and temperature rise of the near-wheel motor. The experimental results verify the rationality of the design scheme.**

***Keywords*— electric vehicles ; axial flux ; torque pulsation; eddy current loss; field weakening**

I. INTRODUCTION

Electric vehicles with electric motor as the driving mechanism, compared with traditional fuel engine cars, have large starting torque and fast acceleration[1], eliminating the gearbox and exhaust emissions in driving, get increasingly used in daily life. At present, the drive system structure of electric vehicles is mainly divided into centralized drive and distributed drive. The centralized drive replaces the conventional fuel engine with a motor which drive two wheels through a differential system to provide power[2]. The distributed drive is powered by multiple motors that can be powered in front or rear of the vehicle in two or four wheels, making the vehicle as a front-wheel drive, rear-wheel drive or four-wheel drive[3]. The distributed drive with a compact structure and flexible layout, shortens the mechanical transmission chain and improves space utilization. The distributed drive improves the driving performance of the vehicle through the differential between the driving wheels, making full use of the vehicle energy, improving the transmission efficiency and increasing the mileage. The distributed drive system, according to the different installation methods of the motor, can be divided into the wheel hub motor drive and the near-wheel motor drive[4]. Compared with the highly integrated wheel hub motor, the near-wheel motor is easy to brake, has good heat dissipation effect, and is more convenient for installation and maintenance. Near-Wheel motors are now used in electric buses, military vehicles, and special transportation vehicles.

The near-wheel drive motor is divided into a radial flux structure and an axial flux structure. The axial length of the axial flux motor is shorter than that of the radial flux machine, so the flattened structure of the axial flux motor is more suitable for wheel mounting. Meanwhile, due to the axial flux motor rotor is light in weight and strong in vibration resistance[5], the service life of the bearing is larger than that of the radial flux motor, thereby improving the reliability of the motor and enhancing the safety and reliability of the new energy vehicle[6]. Although the near-wheel motor improves the operation performance of the electric vehicle, each vehicle needs to be installed with multiple motors and controllers, which complicates the system[7]. At the same time, the near-wheel motor increases the cost of the car and has high requirements for the control technology of the vehicle, such as power balance, electronic differential, energy recovery. The electric vehicle with near-wheel driving requires the motor itself to be small in size, light in weight, small in cogging torque, high in efficiency, large in overload capacity and wide speed range[8].

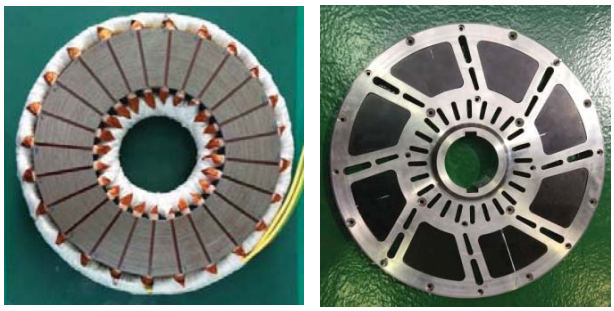

(a) *Stator* (b) Rotor

Fig. 1. Axial flux permanent magnet near-wheel motor

This paper designs a 36KW/5600rpm near-wheel motor for distributed drive electric vehicle. First, the performance parameters of the near-wheel motor is determined. Then the finite element method is used to design the electromagnetic and structure of the motor. Finally, the prototype of near-wheel motor is produced. The efficiency characteristics, field weakening and temperature rise experiments of the motor are carried out.

II. ELECTROMAGNETIC DESIGN

This section gives the electromagnetic design process of the axial flux permanent magnet near-wheel motor, the main parameters of the motor is shown in Table1.

978-1-7281-1675-4/19/$31.00 ©2019 IEEE

TABLE I Specification of the near-wheel motor

Parameter	Value	Parameter	Value
Rated voltage	600VDC	Rated power	36KW
Rated speed	5600rpm	Rated torque	61.4N.m
Rated current	75A	Weight	≤ 42KG
Speed sensor	Resolver	Max power	56KW
Overload time	1 min	Max torque	180N.m
Cooling	Water cooling	Max speed	7500rpm
Max efficiency	⩾93%	Temp Sensor	PT 100

A. Design of Stator

The axial flux permanent magnet near-wheel motor adopts a double-stator and single-rotor structure, which has a small moment of inertia and good heat dissipation conditions. The near-wheel motor, cooled by water, can increase the load capacity. According to the motor formula[9], it can be seen that increasing the motor electrical load can effectively reduce the motor volume. Therefor, the outer diameter of the stator is designed to be 220mm, the inner diameter is 120mm, the axial length of the stator is 44.3mm, the air gap length is 2.2mm, the rotor thickness is 11mm, and the silicon steel sheet is 35DW300.

The slotless structure of the stator core can effectively reduce the cogging torque of the motor, but there are more eddy current losses, which is not conducive to speed regulation and has a small constant power range. Stator core slotting can increase the inductance of the motor, thereby increasing the speed control capability of the motor. Magnetic wedge is used to reduce the tooth groove effect caused by grooving. Therefore, the axial flux permanent magnet near-wheel motor stator adopts slot structure.

The number of stator slots of an axial flux permanent magnet motor is limited by the size of its inner diameter. If the number of stator slots is too large, the tooth width at the inner diameter of the stator is too small, and the accuracy of the silicon steel sheet is difficult to ensure. At the same time, the rigidity of the inner diameter tooth is too small to support the winding coil, and the magnetic circuit saturation may occur, which affects the mechanical performance of the motor. Combined with the above analysis, the axial flux permanent magnet near-wheel motor finally determines the pole slot to match the 8-pole 24-slot structure. The stator slots are evenly distributed on the circumference, and the slot mechanical angle: a = 360°/Z=15°, slot electrical angle: e = p* 360°/Z=60°, pole distance τ= Z /2p= 3, the number of slots per phase per pole q = z/2pm = 1. The stator slot structure is shown in Fig. 2.

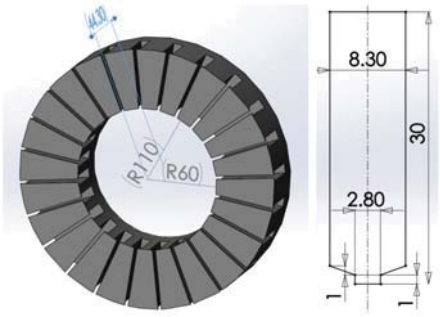

Fig. 2. The parallel grooves stator

Single-layer windings of stator require less coils, no need for insulation between layers, high space utilization rate in the slot, and simple manufacture technology. However, the short-distance ratio (pitch/pole pitch) of the single-layer winding is 1, so the magnetic field waveform is poor, the high-order harmonic magnetic field is strong, which lead to large iron loss and noise, poor starting performance. Single-layer windings are typically used in small capacity motors. Double-layer windings require interlayer insulation, and the space utilization in the slots is low. However, the double-layer winding can improve the magnetic field waveform by selecting a suitable short-range ratio (usually 0.8) to weaken the high-order harmonic field. Meanwhile,the double-layer winding can realize the structure of fractional groove and variable pole. The electromagnetic performance, force index and starting characteristics of the motor using the double-layer winding are better than the single-layer winding, and the double-layer winding saves the wire. Therefore, the axial flux permanent magnet near-wheel motor adopts double-layer winding structure.

B. Design of Rotor

The permanent magnet of the axial flux motor is mounted in a non-magnetic material fixed bracket. The heat of the permanent magnet is mainly dissipated through the air gap. It is necessary to reduce the rotor eddy current loss as much as possible during the design process, otherwise the permanent magnet will be irreversibly demagnetized under a excessive temperature rise. In this paper, the segmented permanent magnet structure is used to suppress the eddy current loss of permanent magnets. The eddy current distribution in the permanent magnet with different block modes is obtained through simulation, as shown in FIG. 3.

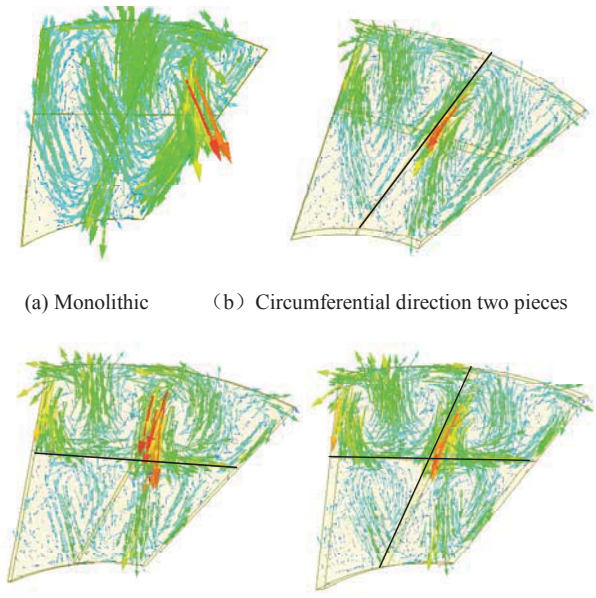

(a) Monolithic (b) Circumferential direction two pieces

(c) Radial direction two pieces (d) Four pieces

Fig. 3. Eddy current distribution in permanent magnet

It can be seen from Fig. 3(a) that the eddy current distribution of the monolithic permanent magnet presents two vortices. Fig.3(b) and 3(c) show the eddy current distribution diagram of a permanent magnet divided into two pieces in the circumferential direction and the radial direction. The eddy current density is significantly reduced compared to the monolithic permanent magnet. FIG.3(d) shows the eddy current distribution pattern when the permanent magnet is divided into four pieces, which is similar to the effect when the permanent magnet is divided into two pieces in the radial direction. It can be concluded that the permanent magnets are divided in the radial direction to reduce the eddy current loss of the permanent magnet of the axial flux motor, which is similar to that the division of the permanent magnets in the axial direction can reduce the eddy current loss of the permanent magnet of the radial flux motor.

Permanent magnet motor stator slotting inevitably produces cogging torque, causing torque and speed fluctuations, and brings noise and vibration. The radial flux motor usually suppresses the cogging torque pulsation through the skewed slots. The axial flux motor stator chute process is complicated, and the installation of auxiliary slots or permanent magnets on the stator increases the manufacturing cost. The cogging torque of axial flux motor is suppressed mainly by skewing permanent magnet. As shown in Fig.4 (the front skew angle is a, the rear skew angle is Δa). At the same time, the optimal pole arc coefficient is selected to reduce the THD (Total Harmonic Distortion) of back electromotive force, and to reduce the commutation torque fluctuation.

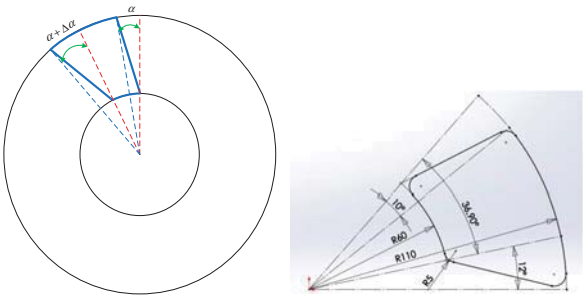

Fig. 4. Skewing permanent magnet

The near-wheel motor is modeled by finite element software. The stator slot and permanent magnet parameters are shown in Table III. The combination of the polar arc coefficient as and the skew angle of the permanent magnet is used to analyze THD of the line and phase back EMF(electromotive force). As shown in Fig.5 The THD of the phase back EMF is generally smaller than the THD of the line back EMF. As the polar arc coefficient as decreases, the THD of the phase and line back EMF increases. With the front skew angle is changed from 8° to 14°, the THD of phase back EMF is first reduced and then increased, The THD value is minimum when front skew angle is 10°. With the rear skew angle is changed from 0° to 8°, the THD of phase back EMF have the same trend, the THD value reaches the minimum point when the rear skew angle is 2°.

TABLE III Parameters of stator slot and permanent magnet

Parameter	Value	Parameter	Value
Slot Opening	2.8mm	Magnet thickness	11mm
Slot depth	28mm	Magnet material	N35UH
Slot width	8.3mm	Winding type	Wye
Tooth Tip Angle	20°	Conductors number	38
Parallel Branches	2	Spacer factor	0.72

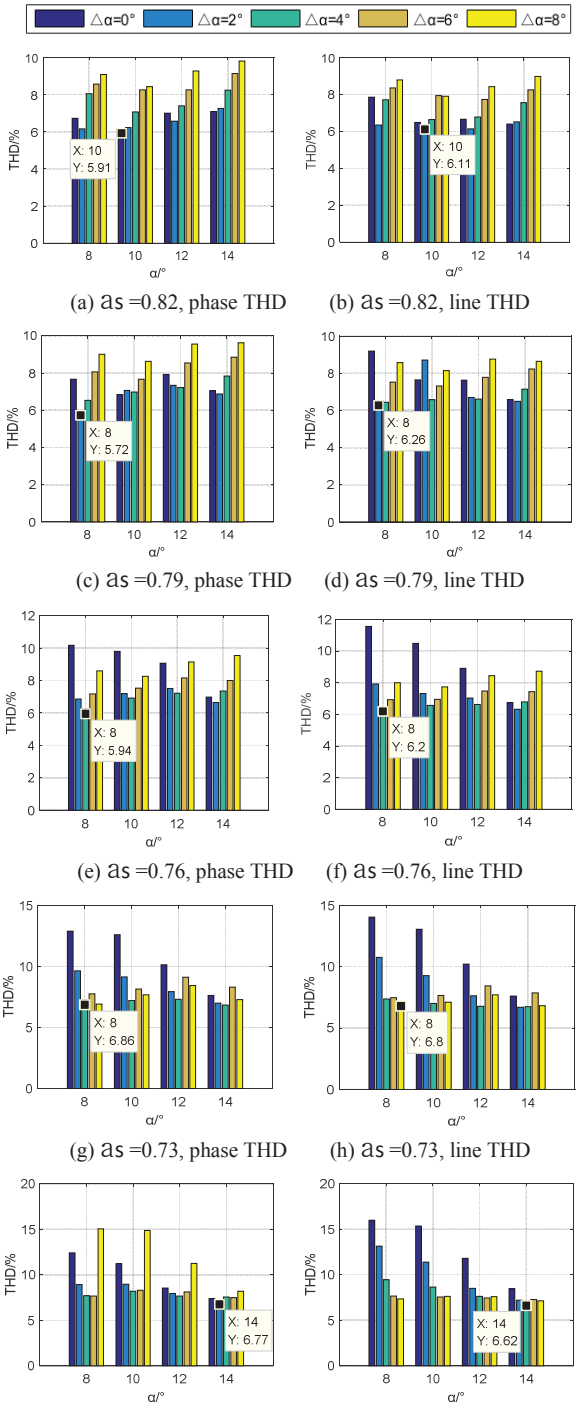

(a) as =0.82, phase THD (b) as =0.82, line THD

(c) as =0.79, phase THD (d) as =0.79, line THD

(e) as =0.76, phase THD (f) as =0.76, line THD

(g) as =0.73, phase THD (h) as =0.73, line THD

(i) as =0.70, phase THD (j) as =0.70, line THD

Fig. 5. THD of the phase and line back EMF

According to the above parameter analysis, it is determined that the polar arc coefficient as of the permanent magnet is 0.79, the front skew angle a is 10°, and the rear skew angle Δa is 2°, as shown in FIG. 4 . The

simulated back electromotive force waveform of the axial flux permanent magnet near-wheel motor at the rated load is shown in FIG. 6(a) and (b). The magnetic density distribution of stator core and permanent magnet is shown in FIG.6(c) and (d), and the electromagnetic torque waveform is shown in FIG. 6(e).

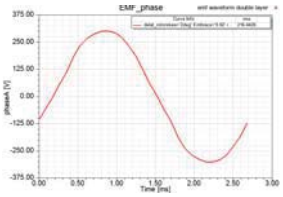

(a) phase back EMF

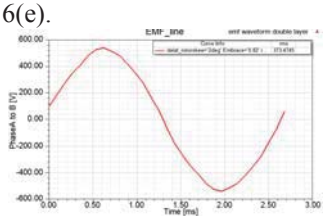

(b) line back EMF

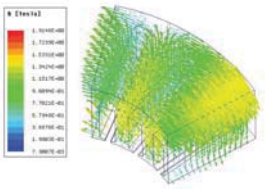

(c) Magnetic field of stator core

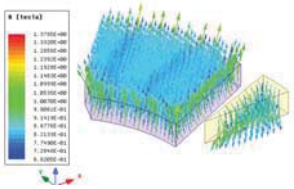

(d) Magnetic field of magnet

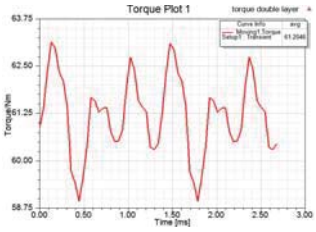

(e) Electromagnetic torque

Fig. 6. Simulated waveform at rated load

C. *Thermal design*

Electric vehicles require a large overload capacity of the motor, and a large temperature rise is usually caused when the motor is overloaded. The high temperature of the motor will accelerate the aging of the insulating material. Excessive temperature will cause irreversible demagnetization of the permanent magnet and affect the service life of the motor. In order to obtain high overload capacity and power density, the axial flux permanent magnet near-wheel motor uses water cooling to dissipate heat. The heat generated by the stator windings and the core is dissipated through the spiral water passages on the front and rear end cover. FIG.7 is a schematic diagram of a spiral waterway water cooling system, the number of spiral channels is 5 and the width of the channel is 10 mm.

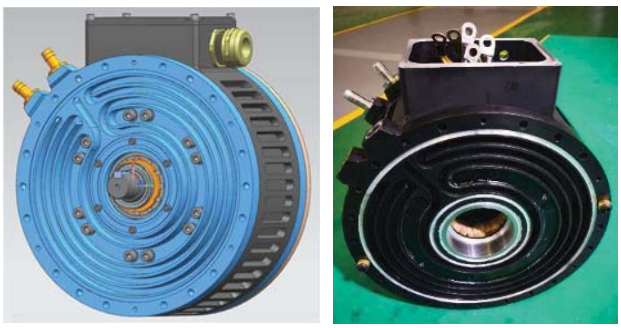

Fig. 7. Spiral water passages

The finite element method is used to analyze the three-dimensional temperature field of the near-wheel motor. Because the near-wheel motor adopts a double-stator with an 8-pole 24-slot structure, its spatial structure has axis symmetry, so it is only necessary to establish a model under one magnetic pole. The thermal property of the near-wheel motor are shown in Table IV.

Table IV Material thermal properties

Component	Thermal conductivity / W·(m·K)$^{-1}$			Specific heat cap/J·(kg·K)$^{-1}$
	Radial	Tangential	Axial	
Stator core	4.3	35	35	502.4
Air	0.029	0.029	0.0029	1005
Coils	223	0.63	0.63	654
Insulator	0.21	0.21	0.21	1700
Magnet	9	9	9	440
Shell	210	210	210	871
Slot wedge	0.2	0.2	0.2	1500

The temperature field load of the near-wheel motor at the rated load is shown in FIG. 8(a), the inlet cooling water flow is 12L/min, and the ambient temperature is 60℃. The temperature distribution of the near-wheel motor obtained by simulation is shown in FIG. 8(b)-(d). The highest temperature of winding is 109℃, and the average temperature is 99℃. The maximum temperature of permanent magnet is 135℃, which is located in the middle of permanent magnet, and the average temperature is 127℃.

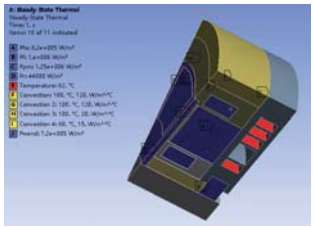

(a) Temperature field load

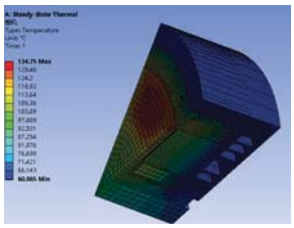

(b) Motor

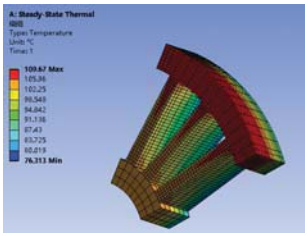

(c) Winding

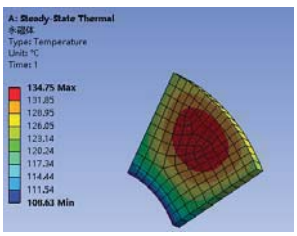

(d) Permanent magnet

Fig. 8. Temperature rise distribution

After the temperature of the near-wheel motor at the rated load is stable , continue to operate at the maximum load for 1min. Simulation results show that the maximum temperature of the motor winding is 171℃, and the maximum temperature of the permanent magnet is 140℃. It can be seen that the temperature of permanent magnet changes very little when it is temporarily overloaded. The maximum temperature of the motor rises to 178 °C, and the insulation specification is 200 °C, which meets the requirements of the index.

III. PROTOTYPE AND EXPERIMENT

A. The experiment platform

The experiment platform of the near-wheel motor is shown in FIG.9. The power cabinet rectifies the external three-phase ac power supply into dc power supply. On the one hand, it supplies power to the near-wheel motor controller, on the other hand, it supplies the inverter to control the variable frequency motor as a load for the near-wheel motor. The power analyzer EV3000 has four measuring channels, one of which measures the DC bus voltage and current of the near-wheel motor controller, and the other three channels measures the voltage and current of the three-phase winding of the near-wheel motor. The torque and speed sensors measure the output of the near-wheel motor. The measurement signal is transmitted to the master compute through the network cable, and the master compute displays the value and waveform of the measurement data. The near-wheel motor and controller are cooled by circulating water.

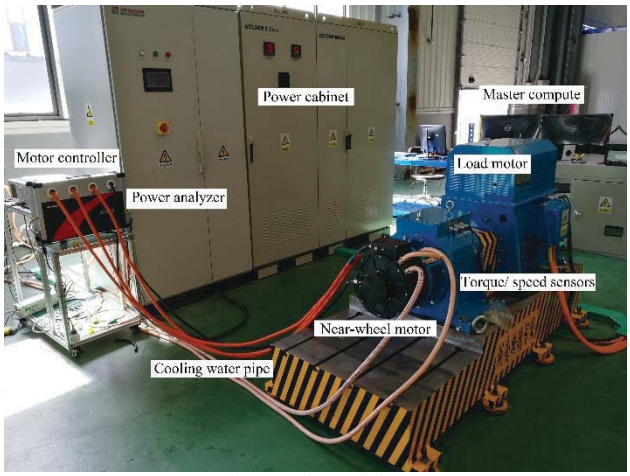

Fig.9. Experiment platform

B. Motor efficiency test

Set the circulating water-cooled water flow rate to 12L/min, the input water temperature to 30°C, the controller bus voltage of the near-wheel motor to 600V, the rotational speed from 100rpm to 6500rpm, the speed interval is 100rpm. Test the voltage and current values of the motor and the controller at each speed with the torque increase from 0 to the rated torque.

FIG. 10(a) shows the performance of the near-wheel motor and controller at rated power (36 kW, 5600 rpm, 61 N.m). It can be seen that the controller efficiency is 98.05% at rated power, the motor efficiency is 94.93%, and the system efficiency is 93.08%. The motor line voltage, phase current, and torque waveform are as shown in FIG.10(b), which is close to the simulated waveform. FIG.10(c) shows the performance of the near-wheel motor and controller at a load power of 60.8 kW (over 56 kW peak). The motor speed is 5600 r/min, the controller efficiency is 98.13%, the motor efficiency is 94.27%, and the system efficiency is 92.51%.

The efficiency MAP of the near-wheel motor is shown in FIG.10(d), in which the high efficiency zone of the motor is in the working condition of rated power above 36kW, the highest efficiency is over 93.78%, and the area with efficiency greater than 90% accounts for more than 70% of the total working conditions.

(a) Rated power of 36 kW, 5600 rpm, 61 N.m

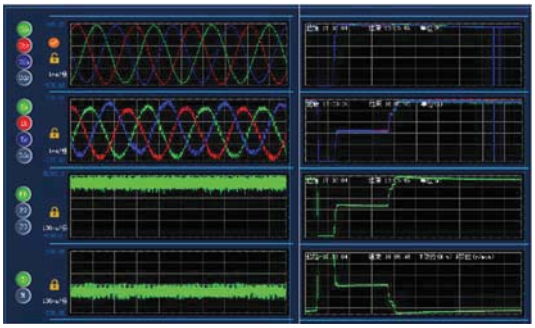

(b) Line voltage, phase current, and torque waveform

(c) Load power of 60.8 kW, 5600 r/min

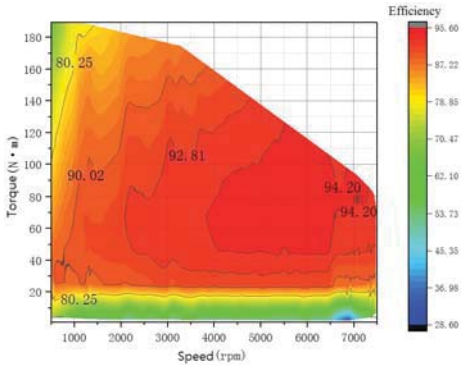

(d) Efficiency MAP

Fig. 10. Experimental result of the near-wheel motor

C. Field weakening test

The maximum speed of the near-wheel motor is 7500 rpm. When the motor speed is above 6500 rpm, it is necessary to increase the demagnetization current to continue to increase the motor speed. FIG.11 shows the curve of demagnetization current as the power is increased at 6600 rpm, 7000 rpm and 7500 rpm. It can be seen from the figure that the demagnetization current increases from 0A to 10A when the motor speed is 6600 rpm. If the motor speed exceeds 7000 rpm, the demagnetization current needs to be applied from the beginning, and increases from 15A to 35A as the power increases. At a maximum speed of 7500 rpm, the demagnetization current begins with a 35A current and eventually increases to 50A.

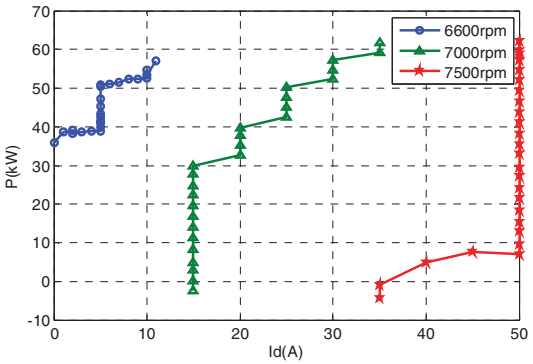

Fig. 11. Demagnetization current

D. Temperature rise test

Set the water flow rate to 12L/min, the control input water temperature is controlled at 60 °C, the near-wheel motor runs under the rated load, and the test time is one hour. The temperature rise of the motor is measured by PT100 sensor. At the beginning of the test, the initial temperature of the motor was 28 °C. As time went on, the motor temperature gradually increased. After half an hour, the motor temperature rose to 113 °C, and then the temperature no longer rises. The highest temperature rise meets the requirements.

V. CONCLUSION

In this paper, an axial flux permanent magnet near-wheel motor is proposed for the distributed drive system of electric vehicles. Electromagnetic design, heat dissipation design, structural design and experimental verification are carried out. The following conclusions are drawn: Although the near-wheel motor is not as compact as the hub motor, it is easy to manufacture and easy to maintain. The permanent magnets are divided in the radial direction to reduce the eddy current loss of the permanent magnet of the axial flux motor. Water cooling can improve the overload capacity of the near-wheel motor. Structural strength and prevention of resonance are taken into account when designing the motor in a lightweight design.

References

[1] X. Zhang, D. Göhlich and J. Li, "Energy-Efficient Toque Allocation Design of Traction and Regenerative Braking for Distributed Drive Electric Vehicles," in IEEE Transactions on Vehicular Technology, vol. 67, no. 1, pp. 285-295, Jan. 2018.

[2] N. Mutoh, "Driving and Braking Torque Distribution Methods for Front- and Rear-Wheel-Independent Drive-Type Electric Vehicles on Roads With Low Friction Coefficient," in IEEE Transactions on Industrial Electronics, vol. 59, no. 10, pp. 3919-3933, Oct. 2012.

[3] X. Yuan and J. Wang, "Torque Distribution Strategy for a Front- and Rear-Wheel-Driven Electric Vehicle," in IEEE Transactions on Vehicular Technology, vol. 61, no. 8, pp. 3365-3374, Oct. 2012.

[4] R. Wrobel, J. Goss, A. Mlot and P. H. Mellor, "Design Considerations of a Brushless Open-Slot Radial-Flux PM Hub Motor," in IEEE Transactions on Industry Applications, vol. 50, no. 3, pp. 1757-1767, May-June 2014.

[5] W. Yu and C. Gu, "Dynamic analysis of a novel clutch system for in-wheel motor drive electric vehicles," in IET Electric Power Applications, vol. 11, no. 1, pp. 90-98, 1 2017.

[6] D. Tan and C. Lu, "The Influence of the Magnetic Force Generated by the In-Wheel Motor on the Vertical and Lateral Coupling Dynamics of Electric Vehicles," in IEEE Transactions on Vehicular Technology, vol. 65, no. 6, pp. 4655-4668, June 2016.

[7] M. Aydin and M. Gulec, "A New Coreless Axial Flux Interior Permanent Magnet Synchronous Motor With Sinusoidal Rotor Segments," in IEEE Transactions on Magnetics, vol. 52, no. 7, pp. 1-4, July 2016

[8] S. Javadi and M. Mirsalim, "A Coreless Axial-Flux Permanent-Magnet Generator for Automotive Applications," in IEEE Transactions on Magnetics, vol. 44, no. 12, pp. 4591-4598, Dec. 2008.

[9] M. Sadeghierad, H. Lesani, H. Monsef and A. Darabi, "High-speed axial-flux permanent-magnet generator with coreless stator," in Canadian Journal of Electrical and Computer Engineering, vol. 34, no. 1/2, pp. 63-67, Winter-Spring 2009.

[10] P. Jin, Y. Yuan, Q. Xu, S. Fang, H. Lin and S. L. Ho, "Analysis of Axial-Flux Halbach Permanent-Magnet Machine," in IEEE Transactions on Magnetics, vol. 51, no. 11, pp. 1-4, Nov. 2015